

Spectral characteristics of 2-(2'-aminophenyl)benzimidazole in β -cyclodextrin

Swadeshmukul Santra, Sneha K. Dogra *

Department of Chemistry, Indian Institute of Technology, Kanpur, Kanpur-208016, India

Received 10 October 1995; accepted 17 April 1996

Abstract

The spectral characteristics of 2-(2'-aminophenyl)benzimidazole (2-APBI) were studied as a function of the β -cyclodextrin (β -CDx) concentration in aqueous medium and the time. The fluorescence quantum yields and fluorescence decay times were also determined. The results indicate that 2-APBI forms a 1 : 1 inclusion complex with β -CDx. The absorption and fluorescence spectra are shifted to the red. The increase in the fluorescence quantum yield of the normal Stokes-shifted band is attributed to the decrease in the non-radiative decay rate constant. The decrease in the fluorescence quantum yield of the large red-shifted fluorescence band is due to back proton transfer from the β -CDx hydroxyl groups to the imine group to yield the amine group in the S_1 state. It is also concluded that the pyridine nitrogen atom and the amino nitrogen are present near the larger rim of β -CDx.

Keywords: 2-(2'-Aminophenyl)benzimidazole; β -Cyclodextrin; Spectral characteristics

1. Introduction

Cyclodextrins form inclusion complexes [1] with organic molecules in aqueous solutions. The binding force [2,3] behind complex formation involves hydrogen bonding, van der Waals' forces or hydrophobic interactions. Complexation of the guest molecule occurs within the hydrophobic cavity, and the glucose hydroxyl groups at both entrances of the cyclodextrin cavity further stabilize complex formation via hydrogen bonding. In many ways, cyclodextrins are better systems than micelles, because they form stable systems, whereas micelles are transitory and are in dynamic equilibrium with the monomer surfactant molecules from which they are formed. The formation of inclusion complexes with cyclodextrins can be compared with the solubilization of non-polar solute molecules in micelles [4].

Since the fluorescence spectral characteristics of certain molecules are very sensitive to their surroundings, environments in structured microheterogeneous [5,6] systems can play a major role in the alteration of these properties, and molecules can be used as probes to study the properties of microheterogeneous systems. This study concentrates on the photophysics of 2-(2'-aminophenyl)benzimidazole (2-APBI) in aqueous solutions of β -cyclodextrin (β -CDx). An earlier study [7] on 2-APBI has shown that the dual fluores-

cence is very sensitive to specific interactions; therefore the spectral characteristics of 2-APBI studied in β -CDx can provide information on the location and environment around this molecule in β -CDx.

2. Materials and methods

2-APBI was obtained from Aldrich Chemical Company and was purified by recrystallization from methanol. The purity was checked by thin layer chromatography (TLC) (single spot) and by the similar fluorescence spectral bands obtained on excitation at different wavelengths. β -CDx was also obtained from Aldrich Chemical Company and was used as received. AnalaR grade methanol (E. Merck) was further purified as described in the literature [8]. Triply distilled water was used to prepare aqueous solutions. A stock solution of 2-APBI was prepared in methanol. The final concentration of 2-APBI for recording the spectra, evaluating ϕ_f and determining the excited state lifetime was 1×10^{-5} M, containing less than 1% (v/v) methanol.

The instruments used to record the absorption and fluorescence spectra and to determine the lifetimes and the procedures used to determine ϕ_f have been described elsewhere [9–11].

* Corresponding author.

Table 1

Absorption band maxima (λ_{ab} (nm)), fluorescence band maxima (λ_n (nm)) and fluorescence quantum yield (ϕ_n) of a fresh solution of 2-APBI in β -CDx and after 9 and 24 h; [2-APBI] = 1×10^{-5} M, λ_{exc} = 305 nm

Sample	[β -CDx] (10^{-3} M)	Fresh			9 h			24 h		
		λ_{ab}	λ_n	ϕ_n	λ_{ab}	λ_n	ϕ_n	λ_{ab}	λ_n	ϕ_n
1	0.0	320	410	0.36	320	410	0.33	320	410	0.35
2	2.0	320	411	0.35	320	413	0.38	320	414	0.43
3	4.0	320	412	0.34	320	414	0.42	322	413	0.52
4	6.0	321	414	0.37	322	415	0.54	324	417	0.72
5	8.0	321	416	0.43	323	417	0.59	325	418	0.70
6	10.0	322	416	0.48	325	419	0.83	328	418	1.0
7	12.0	323	416	0.50	327	418	0.84	331	418	1.0
8	15.0	325	418	0.59	332	418	1.0	–	–	–

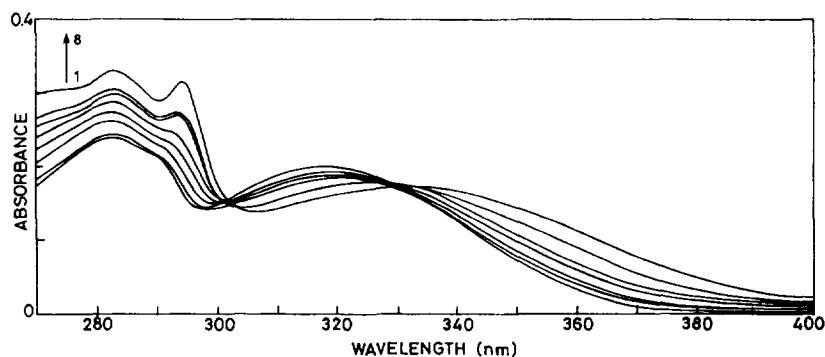


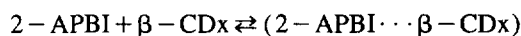
Fig. 1. Absorption spectra of 2-APBI at different [β -CDx] values: 1, 0.0 M; 2, 0.002 M; 3, 0.004 M; 4, 0.006 M; 5, 0.008 M; 6, 0.01 M; 7, 0.012 M; 8, 0.015 M.

3. Results

3.1. Absorption spectrum

Table 1 shows the absorption maximum of the long-wavelength band as a function of the β -CDx concentration. The absorption spectra of 2-APBI recorded at different [β -CDx] values are shown in Fig. 1. Although not shown, the absorption maxima of all the bands, except that at 292 nm, are red shifted, and the red shift observed is largest for the lowest energy transition. The molecular extinction coefficients of all the bands increase with increasing [β -CDx]. The absorption spectra of the solutions were also recorded after 9 h and 24 h. Although red shifts in all the spectral bands can be seen in comparison with those in water, a red shift is only observed in the long-wavelength band of 2-APBI when compared with spectra recorded for fresh solutions containing the same amount of β -CDx. The second band maximum from the lowest energy side becomes structured, and the structure increases with increasing [β -CDx] and with time for a given concentration of β -CDx. The structure of this band resembles that in the spectrum of 2-APBI recorded in solutions of medium polarity solvents or in a solution containing 60% (v/v) dioxan in water. It is described by a vibrational frequency of $1450 \pm 100 \text{ cm}^{-1}$. The absorbances measured at two wavelengths as a function of [β -CDx] are plotted in Fig. 2.

The isosbestic points appearing in the absorption spectrum at 330 nm and 305 nm indicate an equilibrium



The equilibrium constant K defined as

$$K = \frac{[2\text{-APBI} \cdots \beta\text{-CDx}]}{[2\text{-APBI}][\beta\text{-CDx}]}$$

was determined using the procedure of Hamai [12], i.e.

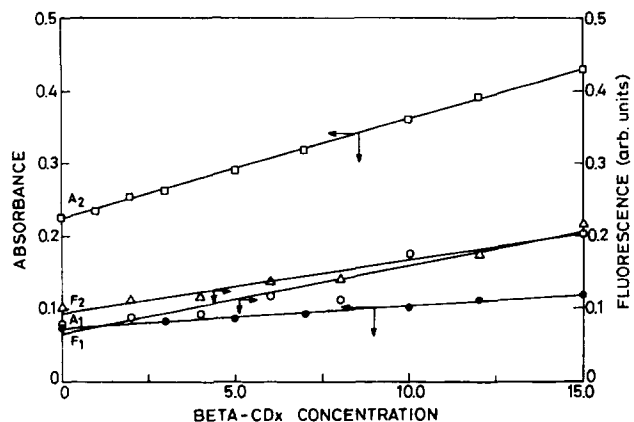


Fig. 2. Plot of absorbance (\bullet , 285 nm; \square , 350 nm) and fluorescence (\circ , 302 nm; \triangle , 330 nm) of 2-APBI vs. [β -CDx]. Fresh solution of [2-APBI] = 1×10^{-5} M.

$$\frac{1}{I - I_0} = \frac{1}{a} + \frac{1}{a[\beta\text{-CDx}]}$$

where I and I_0 are the absorbance or fluorescence intensity in the presence or absence of $\beta\text{-CDx}$ at a given wavelength and a is a constant. The values of K obtained at wavelengths of 270 and 285 nm are 25 M^{-1} and 26.8 M^{-1} respectively, i.e. in good agreement. At wavelengths of 325 and 340 nm, in the long-wavelength band, we obtain a negative value of the intercept and thus a negative value of K . Similarly, we also obtain a negative intercept if the fluorescence intensity at any one particular wavelength is used. This has not been resolved.

3.2. Fluorescence spectrum

Similar to the fluorescence spectrum recorded in water, only one normal Stokes-shifted fluorescence band is observed up to $[\beta\text{-CDx}] = 0.015 \text{ M}$ (the tail part of the fluorescence spectrum is extended at higher $[\beta\text{-CDx}]$ values). The band maximum as a function of $[\beta\text{-CDx}]$ is shown in Table 1 and the fluorescence spectra of 2-APBI in the absence and presence of $\beta\text{-CDx}$ are shown in Fig. 3. The fluorescence band maximum is red shifted and the width at half-maximum height (FWHM) and the fluorescence quantum yield (ϕ_f) increase with increasing $\beta\text{-CDx}$ concentration. The characteristics of the fluorescence spectra after 9 and 24 h are different from those of the absorption spectra, i.e. no change is observed in the fluorescence band maximum, but ϕ_f increases with time for a given concentration of $\beta\text{-CDx}$. The value of ϕ_f nearly doubles after 24 h at $[\beta\text{-CDx}] = 0.012 \text{ M}$, whereas ϕ_f of the solution containing no $\beta\text{-CDx}$ remains almost unchanged. This indicates that the 2-APBI present in aqueous solution does not decompose on keeping, and the increase in ϕ_f in $\beta\text{-CDx}$ is due to the inclusion complex. The fluorescence intensities measured at a given wavelength vs. $[\beta\text{-CDx}]$ are also plotted in Fig. 2. An increase in the absorbance and fluorescence intensity has been observed previously [12–18].

3.3. Fluorescence excitation spectrum

The fluorescence excitation spectra of 2-APBI in freshly prepared $\beta\text{-CDx}$ solution were recorded at five different emission wavelengths at 0.012 M $\beta\text{-CDx}$. The spectra are shown in Fig. 4. It is clear from Fig. 4 that the fluorescence excitation spectrum changes as the emission wavelength is varied. The changes observed in the band maxima in the excitation spectra monitored at 420 and 440 nm are small in comparison with those for spectra monitored at 480 and 500 nm. This indicates that the absorption spectrum includes contributions from different conformers.

3.4. Excited singlet state lifetimes

The lifetimes of freshly prepared solutions of 2-APBI at different concentrations of $\beta\text{-CDx}$ were measured by exciting

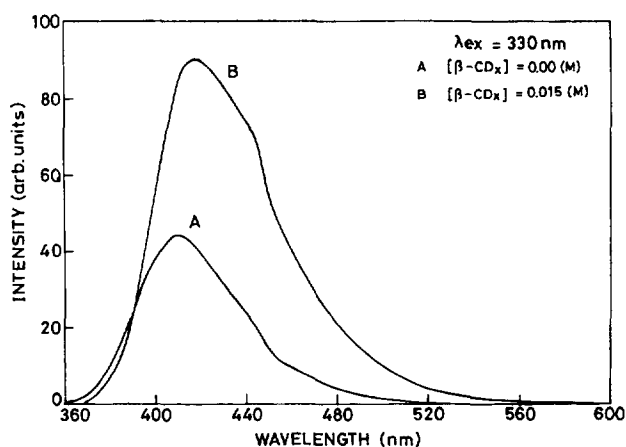


Fig. 3. Fluorescence spectra of 2-APBI in the presence (B) ($[\beta\text{-CDx}] = 0.015 \text{ M}$) and absence (A) of $\beta\text{-CDx}$.

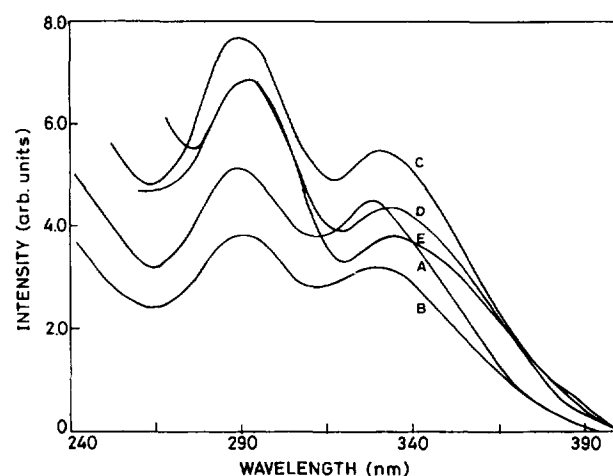


Fig. 4. Fluorescence excitation spectra of 2-APBI in 0.012 M $\beta\text{-CDx}$ monitored at 420 nm (A), 440 nm (B), 460 nm (C), 480 nm (D) and 500 nm (E). $[2\text{-APBI}] = 1 \times 10^{-6} \text{ M}$.

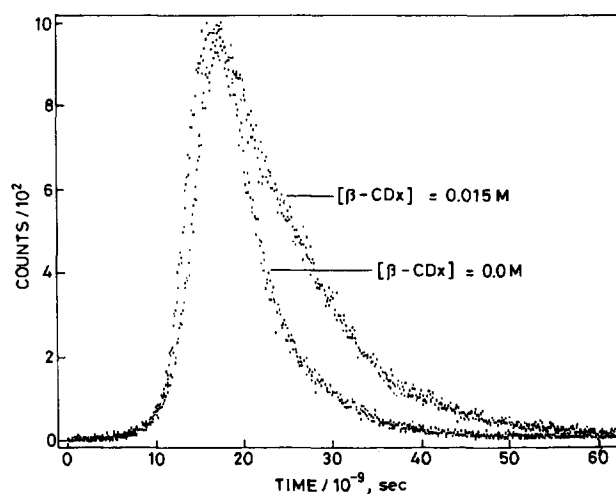


Fig. 5. Fluorescence decay curves of 2-APBI in water and in aqueous solutions of $\beta\text{-CDx}$ at 300 K; $\lambda_{\text{exc}} = 332 \text{ nm}$; $\lambda_{\text{em}} = 418 \text{ nm}$; $[2\text{-APBI}] = 1 \times 10^{-5} \text{ M}$.

the solutions at 332 nm and monitoring at 418 nm. The decay curves, even in the absence of $\beta\text{-CDx}$, follow a second-order exponential decay (Fig. 5). Although the relative amplitudes

Table 2

Lifetimes (ns) and relative amplitudes of the second-order decay; $\lambda_{\text{exc}} = 332$ nm, $\lambda_{\text{em}} = 418$ nm, $[2\text{-APBI}] = 1 \times 10^{-5}$ M

Sample	[β -CDx] (10^{-3} M)	Fresh solution				24 h			
		A_1	A_2	τ_1	τ_2	A_1	A_2	τ_1	τ_2
1	0.0	78.7	21.3	0.39	4.63	76.8	23.2	0.35	4.56
2	2.0	77.2	22.8	0.23	5.37	–	–	–	–
3	4.0	78.8	21.2	0.20	6.29	–	–	–	–
4	6.0	51.6	48.4	0.29	6.82	31.1	68.9	0.40	7.58
5	8.0	42.8	57.2	0.40	7.72	34.0	66.0	0.29	7.52
6	10.0	41.4	58.6	0.28	7.86	28.2	71.8	0.27	7.64
7	12.0	27.4	72.6	0.36	7.68	25.6	74.4	0.28	8.20
8	15.0	22.9	77.7	0.27	7.81	–	–	–	–

Table 3

Lifetimes (ns) and relative amplitudes of second-order decay recorded at different wavelengths for a fresh solution and a solution kept for 24 h; $\lambda_{\text{exc}} = 332$ nm, $[\beta\text{-CDx}] = 0.012$ M, $[2\text{-APBI}] = 1 \times 10^{-5}$ M

Sample	λ_{em} (nm)	Fresh solution				24 h			
		A_1	A_2	τ_1	τ_2	A_1	A_2	τ_1	τ_2
1	418	22.9	77.1	0.27	8.60	25.4	74.6	0.28	8.46
2	440	21.6	78.4	0.27	8.16	18.2	81.8	0.33	8.43
3	465	20.1	79.9	0.30	8.26	17.1	82.9	0.38	8.57
4	490	16.4	83.6	0.38	8.59	16.2	83.8	0.40	8.33

and lifetimes of both components are given in Table 2, the uncertainty in the values of τ_i occur because these values are below the detection limits of the instrument. The results indicate that the relative amplitude (A_1) of the fast decaying component decreases, whereas that (A_2) of the slow decaying component increases, with increasing $[\beta\text{-CDx}]$. The lifetime (τ_1) of the fast decaying component remains almost unchanged, whereas that (τ_2) of the slow decaying component increases, with increasing $[\beta\text{-CDx}]$. The values of τ_2 reach a maximum at $[\beta\text{-CDx}] > 8 \times 10^{-3}$ M. It should be noted that the fluorescence decay curves, when analysed at $t > 30$ ns, nearly follow a single-exponential decay, giving lifetimes similar to τ_2 obtained from the second-order exponential fit. This indicates that the amount of the fast decaying component in the S_1 state is negligible after this time of analysis.

The fluorescence decay curves analysed after keeping the solutions of 2-APBI in $\beta\text{-CDx}$ for 24 h give the same values of τ_1 , τ_2 , A_1 and A_2 as observed for fresh solutions containing $[\beta\text{-CDx}] > 0.008$ M. The only difference between the fresh solutions and those kept for 24 h is that constant τ_2 values are attained at a lower concentration of $\beta\text{-CDx}$ in the latter case.

The fluorescence decay curves of the freshly prepared solutions and those kept for 24 h were also analysed on excitation at 332 nm with monitoring at 418, 440, 465 and 490 nm in 0.012 M $\beta\text{-CDx}$. The results are given in Table 3. The results clearly show that the lifetimes obtained in the different cases are similar, but slightly greater than the values obtained for higher $[\beta\text{-CDx}]$ (Table 2). This indicates that the τ values are independent of the fluorescence wavelength used for monitoring. The values of the radiative (k_r) and non-radiative

Table 4

Values of the lifetime (ns), ϕ_n and radiative and non-radiative decay rate constants for the fresh solutions

Sample	[β -CDx] (M)	ϕ_n	τ_n	k_r (10^8 s $^{-1}$)	k_{nr} (10^8 s $^{-1}$)
1	0.0	0.36	4.63	0.78	1.38
2	0.002	0.35	5.37	0.65	1.21
3	0.004	0.33	6.30	0.52	1.07
4	0.006	0.37	6.82	0.54	0.93
5	0.008	0.43	7.72	0.56	0.74
6	0.010	0.48	7.86	0.61	0.66
7	0.012	0.50	7.69	0.65	0.65
8	0.015	0.59	7.80	0.76	0.52

(k_{nr}) decay rate constants were calculated using the following equations

$$k_r = \phi_n / \tau_n, \quad k_{nr} = 1 / \tau_n - k_r$$

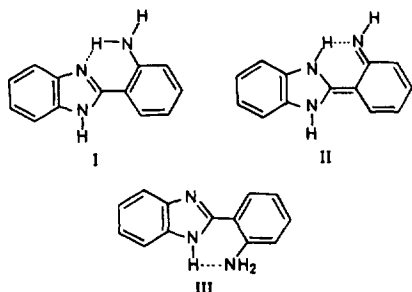
The values obtained are given in Table 4. The data show that the value of k_{nr} decreases with increasing $[\beta\text{-CDx}]$.

4. Discussion

The effects of solvents on the spectral characteristics of 2-APBI have been studied in detail [7]. The results indicate the following: (1) the long-wavelength band in 2-APBI is a composite band and is due to the presence of intramolecular hydrogen bonding leading to structures I and III (see below); (2) the 292 nm band originates from the phenyl ring. The

latter is confirmed by the presence of a similar vibrational structure in 2-phenylbenzimidazole [19] and the substituents present in the phenyl group of 2-phenylbenzimidazole in less polar solvents [20].

The 292 nm band is not very sensitive to the polarity of the solvent, except that the structure disappears in polar/protic solvents. The long-wavelength absorption band maximum is strongly blue shifted, but the spectral shifts observed for the other absorption bands are small, with an increase in the polarity and hydrogen bonding of the solvent. Two fluorescence bands are observed: the short-wavelength band (410 nm) is assigned to structure III and the long-wavelength band (510 nm) to structure II (see below). The first band is red shifted, whereas the second band is blue shifted, with an increase in the polarity and hydrogen bonding of the solvent. ϕ_f of the former band increases slightly and that of the latter decreases drastically (it is very small in methanol and absent in water) with an increase in the polarity and hydrogen bonding of the solvent. The absence of the 530 nm band in water has been attributed to competition between intramolecular and intermolecular hydrogen bonding. In water and other hydrogen bonding solvents, intermolecular hydrogen bonding is predominant, and this decreases the proportion of structure I in water in the S_0 state.

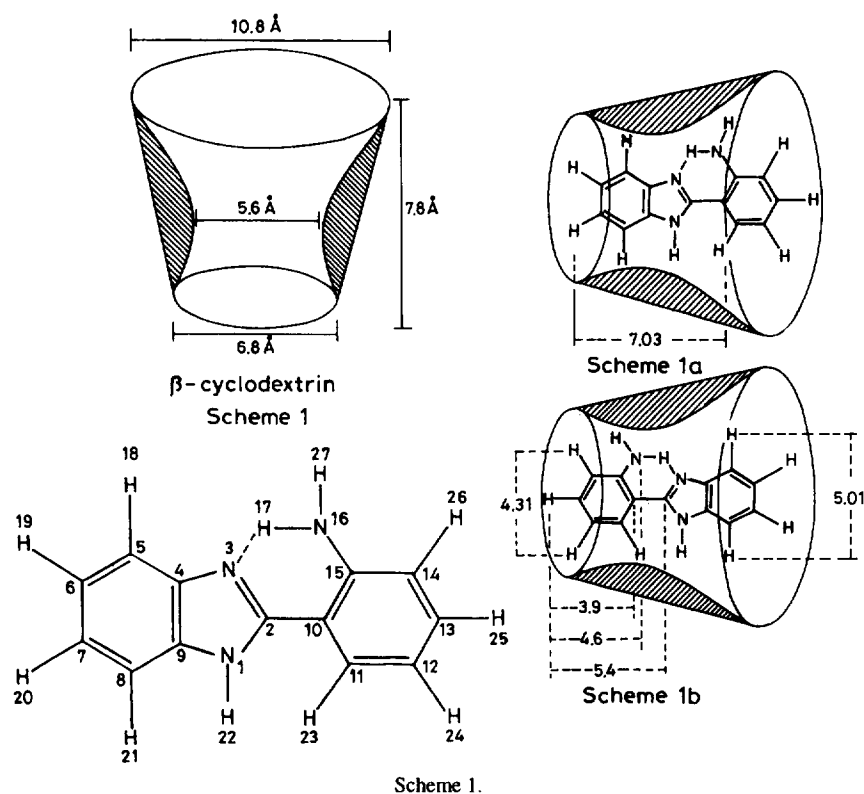


On the basis of the above discussion and considering our results, it is proposed that 2-APBI is transferred from more polar/protic environments (bulk aqueous phase) to less polar/protic environments (cavity of β -CDx), structure I is present in β -CDx although its proportion is not very large and the pyridine nitrogen atom of the benzimidazole moiety and the amino group of the phenyl ring are present near the larger rim of β -CDx. These conclusions are based on the following results.

1. The absorption maximum of the long-wavelength band resembles that observed in methanol and the structure in the 292 nm band is similar to that observed in medium polarity solvents or in a solution containing 60% (v/v) dioxan in water. This confirms the presence of structure I in the β -CDx cavity in the S_0 state. The vibrational frequency ($1400 \pm 100 \text{ cm}^{-1}$) observed in other 2-(amino-phenyl)benzimidazoles [21,22] agrees with the value obtained here and indicates the low polarity environment of the β -CDx cavity.
2. The band maxima observed for the fluorescence excitation spectra recorded at 420 and 440 nm are similar, whereas those recorded at 480 and 500 nm are red shifted in com-

parison with the former. This is because the fluorescence spectra monitored at 420 and 440 nm can be mainly attributed to structure III, whereas the tail part of the fluorescence spectrum (480 and 500 nm) is mainly due to structure I in the S_0 state and structure II in the S_1 state. Thus the absorption spectrum is a mixture of the spectra of these conformers. The increase in the FWHM of the fluorescence spectrum recorded in β -CDx further supports the presence of structure II in the S_1 state, originating from structure I in the S_0 state.

3. The large rim of β -CDx contains 12 secondary hydroxyl groups and thus provides an environment qualitatively similar to poly-hydroxyl alcohols. The red shift observed in the fluorescence spectrum of 2-APBI in β -CDx is not consistent with that observed in methanol or ethanol [7], but agrees with that in glycerol. We could not record the fluorescence spectrum in poly-hydroxyl alcohols.
4. The increase in ϕ_f of the normal Stokes-shifted band with an increase in [β -CDx] is due to the decrease in the quenching rate constant by the solvent molecules as β -CDx provides a protective layer around 2-APBI. This is further substantiated by the data given in Table 4, which show a decrease in the non-radiative decay rate with an increase in [β -CDx] or an increase in the lifetimes of 2-APBI. This type of enhancement in ϕ_f has also been observed by others [12–18].
5. Unlike in methanol or non-polar solvents (where the tautomer II fluorescence band is pronounced), the observation of the tautomer fluorescence band as a shoulder to the main band may be due to the following reasons: (a) 2-APBI forms a 1 : 1 inclusion complex with β -CDx and thus the transferrable protons may not be freely available in the ground state; (b) cyclodextrins are known to be good hydrogen donors [23–25]. In the excited state, the imine structure II, i.e. the double bond between the nitrogen atom and the phenyl ring, undergoes back protonation from β -CDx to give the amine form. This back reaction should increase the decay rate. In other words, ϕ_f and the lifetime of the tautomeric species should decrease in the presence of β -CDx. The appearance of a shoulder substantiates the former, whereas the latter could not be confirmed as the lifetime at this wavelength could not be measured because of the very low intensity. As mentioned above, an increase in the fluorescence intensity of the normal band confirms our earlier conclusion.
6. An increase in ϕ_f of 2-APBI with time at a given concentration of β -CDx is due to the solubilization of 2-APBI in β -CDx and not to a variation in the equilibrium constant with time. This is substantiated by the low value of the equilibrium constant for the inclusion complex between 2-APBI and β -CDx as well as by the achievement of a constant value of ϕ_f at a lower value of [β -CDx] when measured at a longer time. Since the absorption and fluorescence intensities of 2-APBI in a solution of 1% methanol in water (v/v) do not change even after 24 h, it can



be concluded that the fluorophore does not decompose in this medium.

7. The ground state geometry of 2-APBI was optimized using the AM1 method [26] (MOPAC, QCPE program no. 455, version 4.0) on an HP 9000/750 super minicomputer. The vertical distance between H₂₄ and H₂₆ is 5.10 Å, whereas the horizontal distances between H₁₉ and H₂₅ and between H₂₀ and C₁₀ are 10.95 and 7.03 Å respectively. Considering the shape and dimensions of β-CDx (Scheme 1), the only way 2-APBI can enter the β-CDx cavity is lengthwise. Under this situation, and assuming that H₂₀ is present near the lower rim (Scheme 1a), the pyridine nitrogen atom of the benzimidazole ring and the amino group of the phenyl moiety will be present near the larger rim of β-CDx. In no circumstances can 2-APBI be encapsulated completely in the β-CDx cavity (H₂₅–H₁₉ is 10.95 Å). Under such situations, as mentioned above, the inclusion complex will be stabilized by hydrogen bonding via the secondary hydroxyl groups of β-CDx. The red shift in the absorption spectrum substantiates this. We reject the situation in Scheme 1b. Had this been the situation, structure I would have been predominant (the inside of the cavity is non-polar/aprotic) and we would have observed the tautomer fluorescence band near 500 nm with good intensity (not the case here). This is further substantiated by the fact that the distances between H₂₅ and C₁₀, H₂₅ and C₂ and H₂₅ and N₁₆ are 3.9, 5.36 and 4.6 Å respectively, i.e. the pyridine nitrogen and amino group nitrogen would be present in the middle of the β-CDx cavity.

8. The increase in the value of τ_2 with an increase in [β-CDx] is due to the encapsulation of 2-APBI in the β-CDx cavity. Once equilibrium is reached, the values of τ_1 and τ_2 are independent of [β-CDx]. This is substantiated by the fact that τ_1 and τ_2 are similar at different [β-CDx] values when the solutions are analysed after 24 h.
9. We are still uncertain about the nature of the process with regard to the short-lived species. The decay of this species is nearly independent of the concentration of β-CDx, λ_{em} and the time at which analysis is carried out. The fluorescence decay of 2-APBI in *n*-heptane, monitored at 390 nm (band maximum, III), follows a similar behaviour to that observed in water or β-CDx solution (i.e. $A_1=70.8$, $A_2=29.1$, $\tau_1=1.4$ ns, $\tau_2=3.48$ ns). The fluorescence decay of 2-APBI in *n*-heptane, monitored at 530 nm (tautomer band maximum), follows a single exponential with $\tau=0.83$ ns. This value is not very accurate as it is less than the detection limit of the instrument. We cannot assign the fast decay to the rate of intramolecular proton transfer from the amino group to the pyridine nitrogen because this process occurs in the picosecond range, much faster than observed in our case.

Acknowledgements

We thank the Department of Science and Technology, New Delhi for financial support of this work (project no. SP/SI/H-19/91).

References

- [1] M.L. Bender and M. Komiyama, in *Cyclodextrin Chemistry*, Springer, New York, 1978.
- [2] E.S. Hall and J. Ache, *J. Phys. Chem.*, **83** (1979) 1805.
- [3] J.L. Hoffman and R.H. Bock, *Biochemistry*, **9** (1979) 3532.
- [4] H.E. Edwards and J.K. Thomas, *Carbohydr. Res.*, **65** (1978) 173.
- [5] V. Ramamurthy, in V. Ramamurthy (ed.), *Photochemistry in Organized and Constrained Media*, VCH Publishers, New York, 1991.
- [6] K. Kalyanasundaram, in *Photochemistry in Microheterogeneous Systems*, Academic Press, Orlando, FL, 1987.
- [7] A.K. Mishra and S.K. Dogra, *J. Photochem.*, **31** (1985) 333.
- [8] J.K. Riddick and W.B. Bunger, in *Techniques in Organic Chemistry—Organic Solvents*, Wiley-Interscience, New York, 1971, pp. 592, 644, 695.
- [9] J.K. Dey and S.K. Dogra, *J. Phys. Chem.*, **98** (1994) 3638.
- [10] R.S. Sarpal and S.K. Dogra, *J. Chem. Soc., Faraday Trans. I*, **88** (1992) 2725.
- [11] S. Pandey, R.S. Sarpal and S.K. Dogra, *J. Colloid Interface Sci.*, **172** (1995) 407.
- [12] S. Hamai, *J. Phys. Chem.*, **93** (1989) 2074.
- [13] M. Hoshino, M. Imamura, K. Ikehara and Y. Hama, *J. Phys. Chem.*, **85** (1981) 1820.
- [14] S. Hamai, *J. Phys. Chem.*, **93** (1989) 6527.
- [15] S. Hashimoto and J.K. Thomas, *J. Am. Chem. Soc.*, **107** (1985) 4655.
- [16] A. Nakazima, *Spectrochim. Acta, Part A*, **39** (1983) 913.
- [17] K.A. Al-Hassan, U.K.A. Klien and A. Scrwaiyan, *Chem. Phys. Lett.*, **212** (1993) 581.
- [18] S. Kundu, S.C. Bera and N. Chattopadhyay, *Indian J. Chem. A*, **34** (1995) 55.
- [19] A.K. Mishra and S.K. Dogra, *Spectrochim. Acta, Part A*, **39** (1983) 609.
- [20] S.K. Dogra, *Proc. Indian Acad. Sci.*, **104** (1992) 635.
- [21] A.K. Mishra and S.K. Dogra, *Indian J. Phys. B*, **58** (1984) 480.
- [22] A.K. Mishra and S.K. Dogra, *Bull. Chem. Soc. Jpn.*, **58** (1985) 3587.
- [23] N. Chattopadhyay, *J. Photochem. Photobiol. A: Chem.*, **58** (1991) 31.
- [24] M. Senger, in J.L. Atwood, J.E.D. Davies and D.D. MacNicol (eds.), *Inclusion Complexes*, Vol. 2, Academic Press, London, 1984, p. 231.
- [25] G. Porter and M.W. Windsor, *Proc. R. Soc. London, Ser. A*, **245** (1958) 238.
- [26] J. Del Bene and H.H. Jaffe, *J. Chem. Phys.*, **448** (1968) 1807.